TURKISH JOURNAL OF REMOTE SENSING
(Türkiye Uzaktan Algılama Dergisi)
e-ISSN 2687-4997
https://dergipark.org.tr/en/pub/tuzal

Deformation analysis of embankment dam using field survey and multisensor InSAR time-series: A case study of Mosul Dam, Iraq

Ahmed Ali Azeez[1], Sadra Karimzadeh[*2], Khalil Valizadeh Kamran[3], Masashi Matsuoka[4]

[1] *University of Tabriz, Faculty of Planning and Environmental Sciences, Department of Remote Sensing and GIS, Tabriz, Iran; ahmedalshihmani@yahoo.com*
[2] *University of Tabriz, Faculty of Planning and Environmental Sciences, Department of Remote Sensing and GIS, Tabriz, Iran; sa.karimzadeh@tabrizu.ac.ir*
[3] *University of Tabriz, Faculty of Planning and Environmental Sciences, Department of Remote Sensing and GIS, Tabriz, Iran; valizadeh@tabrizu.ac.ir*
[4] *Institute of Science Tokyo, Department of Architecture and Building Engineering, Japan; matsuoka.m.e594@m.isct.ac.jp*

Article History:
Received: 5 May 2025
Revised: 8 June 2025
Accepted: 10 June 2025
Published: 30 December 2025

Abstract: Effective water resource management is crucial in Iraq's arid climate, particularly concerning the Tigris and Euphrates rivers. The Mosul Dam, one of the country's largest and most important infrastructures, plays a vital role in water supply and flood control. This study investigates structural displacement in Mosul Dam using three data sources: (1) field surveys with conventional instruments, and (2) synthetic aperture radar (SAR) images from Sentinel-1 and (3) ALOS-2 PALSAR-2 SAR images. The SAR data were processed using the SAR interferometric (InSAR) Small Baseline Subset (SBAS) technique. Analysis reveals that the central section of the dam experiences the most significant subsidence, whereas the lateral sections show relatively minor deformation. Field survey data from November 2013 to May 2024 indicate an average subsidence velocity of 2.82 mm/year, with a cumulative rate of 28.94 mm and a maximum recorded subsidence of 97.45 mm. SBAS analysis of Sentinel-1 data (November 2015–April 2024) shows an average subsidence velocity of 2.31 mm/year, with cumulative and maximum subsidence values of 15.52 mm and 74.40 mm, respectively. Similarly, SBAS analysis of ALOS-2 data (November 2014–March 2024) indicates an average subsidence velocity of 2.98 mm/year, with a cumulative rate of 14.37 mm and a maximum of 51.70 mm. Despite some variation in values among the datasets, the annual subsidence rates are closely aligned. All analyses consistently highlight two key findings: (1) the central section of the dam is most prone to subsidence, and (2) there is a distinct difference in displacement patterns (uplift and subsidence) between the central and lateral sections. These insights are critical for understanding the dam's structural behavior and informing future management strategies to ensure its safety and functionality.

Keywords: InSAR; ALOS-2 PALSAR-2; Sentinel-1; subsidence; SBAS; field surveys; Mosul Dam

Citation: Azeez, A. A., Karimzadeh, S., Kamran, K. V., & Matsuoka, M. (2025). Deformation analysis of embankment dam Using field survey and multisensor InSAR time-series: A case study of Mosul Dam, Iraq. *Turk. J. Remote Sens.*, 7(2), 244-262. https://doi.org/10.51489/tuzal.1690530

1. Introduction

Land subsidence can occur at any time and place around the globe, often progressing slowly when severe. This phenomenon can lead to disasters for humans, including dam collapses, road failures, and structural cracks and damage to buildings. Therefore, studying land subsidence in dams and urban areas can help us better understand and manage the risks associated with such disasters (Cigna & Tapete, 2021; Gheorghe & Arma, 2016). Dams play a pivotal role in harnessing the potential of water resources, especially in arid and flood-prone areas where population growth and migration have increased the demand for water storage, flood control, electricity generation, irrigation, navigation, and recreation (ASDSO, 2023; Gracon LLC, 2003). The Mosul Dam (subject of our study) is considered the largest dam in Iraq. The soil below the dam consists of rocks, including marls, chalky limestone, gypsum, anhydrite, clays, and severely fractured limestone. Most of the rocks below the dam are

soluble and the development of karst features formed after rock dissolution, creating subsurface cavities that cause the loss of support of the overlying material and result in a collapse feature recognizable at the surface (Bowen, 2007). Published studies on Mosul Dam deformation monitoring using DInSAR methods like small baselines (SBAS) and PSI lack verification through in-situ data collection (Othman, et al. 2.019).

Land subsidence monitoring, particularly at reservoirs and dam sites, plays a vital role in mitigating geohazards (Sica & Pagano, 2009). Most SAR satellite missions, such as TanDEM-X (TDX)/PAZ, COSMO-SkyMed (CSK), and Sentinel-1A/B, are designed as constellations that enhance spatial coverage and enable faster data acquisition, facilitating timely monitoring of natural events and disasters (Milillo et al., 2016). Differential Interferometric Synthetic Aperture Radar (DInSAR) is a powerful technique for detecting ground deformation with millimetric accuracy for Landslides caused by earthquakes, volcanoes activity, and structural subsidence in human-made infrastructure like dams and transportation networks (Wang, et al., 2021) By constructing Interferograms Which are images created by comparing the phase differences between two Synthetic Aperture Radar (SAR) images acquired at different times over the same area (Gabriel et al., 1989). These phase differences reveal subtle changes in ground elevation or movement, allowing scientists to detect surface deformation such as land subsidence with high precision (Martire et al., 2014). Although atmospheric effects and temporal decorrelation can influence data quality, accurate deformation measurements are achievable by focusing on stable targets, known as Permanent Scatterers (PS), which serve as reference points to monitor long-term terrain motion (Ferretti et al., 2000). In recent years, numerous studies have employed SAR techniques to assess dam structural integrity, highlighting their accuracy and sensitivity in displacement detection (Mazzanti et al., 2015; Milillo et al., 2016; Roque et al., 2015; Tomás et al., 2013; Wang et al., 2010;). The Small Baseline Subset (SBAS) technique improves phase coherence and reduces spatial decorrelation by analyzing interferograms from SAR images with short temporal and spatial baselines. It enables accurate reconstruction of ground deformation over time (Barone et al., 2025; Brunson et al., 2020;). SBAS-InSAR has proven effective in monitoring volcanic activity, mining deformation, and dam stability, capturing non-linear surface movements and structural shifts related to water dynamics (Emadali et al., 2017; Gama et al., 2019; Zhou et al., 2016). When combined with GIS, SAR data enhances spatial analysis and supports early detection of hidden structural issues, complementing traditional methods like total stations and GPS (Karimzadeh et al., 2024).

This study applies the SBAS-InSAR technique to assess displacement rates at Mosul Dam using ALOS-2 (L-band) and Sentinel-1 (C-band) SAR imagery, alongside historical elevation data collected periodically by the General Authority for Survey in Iraq. The core objective is to compare and validate ground subsidence results from radar processing with those from field surveys. Although global studies highlight the strengths of L-band (better penetration and coverage in rural areas) and C-band (higher sampling and coherence), few have directly compared their performance over complex geological settings like Mosul Dam, which is built on soluble rocks such as gypsum and limestone (Li et al., 2023; Yang et al., 2023). These differing sensor characteristics call for a deeper evaluation of their reliability in deformation monitoring. Furthermore, field data remain underutilized due to challenges in aligning them with satellite-based measurements. This study fills that gap by integrating field observations with SBAS-InSAR time series, comparing deformation velocities, and analyzing spatial-temporal subsidence patterns. Given the dam's strategic importance and geological sensitivity, this integrated approach supports more accurate risk assessments and timely mitigation strategies.

2. Study Area

The Mosul Dam is the largest embankment dam in Iraq and one of the largest in the Middle East. It is located on the Tigris River, 50 km northwest of the city of Mosul, the third-

largest city in Iraq (Khafaji & Ben Hamed, 2025), with coordinates 36°37′49″N 42°49′23″E Figure 1. The foundation geology of the dam comprises a layered sequence of rocks, including marls, chalky limestone, gypsum, anhydrite, clays, and severely fractured limestone. Most of the rock layers near and under the Mosul Dam are subject to dissolution and the development of karst features, as a result of these weak foundation conditions, both local and international reports—such as those issued by Iraqi technical teams in collaboration with Soviet experts who participated in the dam's original design—have emphasized the presence of significant risks. This concern was later reinforced by the U.S. Army Corps of Engineers (USACE), which issued a comprehensive report in 2006 describing Mosul Dam as "the most dangerous dam in the world." The report highlighted the necessity of ongoing maintenance through grouting operations, which have been continuously implemented since 1986, just a year after the dam became officially operational, to prevent water seepage beneath the dam structure. (Al-Ansari et al., 2021).

Among the most prominent environmental and temporal factors that must be considered and which may play a crucial role in interpreting the behavior and movement of the dam are the seasonal fluctuations in the water level of the reservoir. The highest water levels typically occur in late spring and early summer, particularly during the months of April to June, as a result of snowmelt from the Turkish highlands that feed the Tigris River, along with precipitation during winter and spring. Conversely, the lowest water levels usually occur in late summer and early autumn, particularly during September to November, due to increased water demand for irrigation and domestic use during the summer, in addition to a decline in the river's natural inflow during that period, These annual variations between filling and drawdown phases lead to changes in hydrostatic pressure exerted on the dam body and its foundation, potentially causing differential settlement, especially in areas with geologically weak foundations(Al-Ansari, 2013).

Another critical factor is that Mosul Dam lies within a relatively active seismic belt and is periodically subjected to low-to-moderate seismic events. Therefore, the influence of seismic activity must also be considered when analyzing and interpreting dam deformations (Al-Ansari, & Adamo, 2016).

It is worth noting that monitoring efforts at Mosul Dam have been ongoing since its inauguration and have constituted an essential component of its operational strategy due to the foundation's geological characteristics. The General Authority for Dams and Reservoirs, under the Iraqi Ministry of Water Resources, has been responsible for monitoring through a network of benchmarks installed along the dam body to observe settlement and deformation. This system also includes pore pressure readings, seepage monitoring via piezometric pipes, geotechnical sensors, and Global Positioning System (GPS) instruments. Additionally, recent studies employing satellite imagery analysis through InSAR (Interferometric Synthetic Aperture Radar) techniques have been introduced, underscoring the scientific value of the current study that integrates both ground-based measurements and multi-source radar data. Subsequently, particularly after 2003, the U.S. Army Corps of Engineers (USACE), in collaboration with international firms such as Washington Group International, assumed a leading role in supporting and enhancing the monitoring system (Al-Ansari, et al., 2020).

Construction of the Mosul Dam started in 1980 and was completed in June 1984. The first reservoir filling took place in the spring of 1985. The embankment was designed by the Swiss Consultants Group and constructed by the German-Italian Mosul Dam Joint Venture (GIMOD). The dam area has been a water-collecting area for more than 10,000 years. It is a large-scale water storage project with numerous significant benefits, such as protection from the risk of flooding, support for urban water supplies, irrigation, and revitalization of aquatic livestock, tourism, and hydroelectric power generation.

Mosul Dam was designed as a multi-purpose dam, including water supply, irrigation, flood control, and power generation Figure 2, the main dam features a 3.4 kilometer (km)-long earth-fill structure, a powerhouse, a bottom outlet, a concrete-lined gated spillway, and

a fuse-plug secondary spillway, the embankment is 113 meters (m) high and composed of zoned earth-fill construction, the total volume of material in the embankment is reported to be approximately 37.7 million cubic meters (m^3). The embankment of the main dam has a crest elevation of 343 m and a crest width of 10 m.

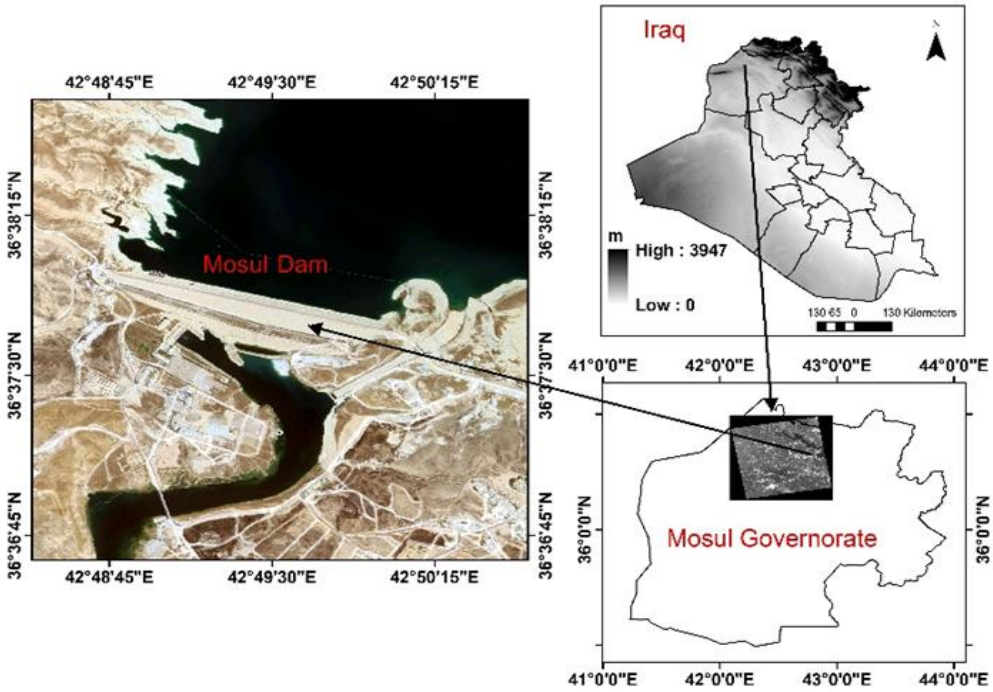

Figure 1. Location of the study area

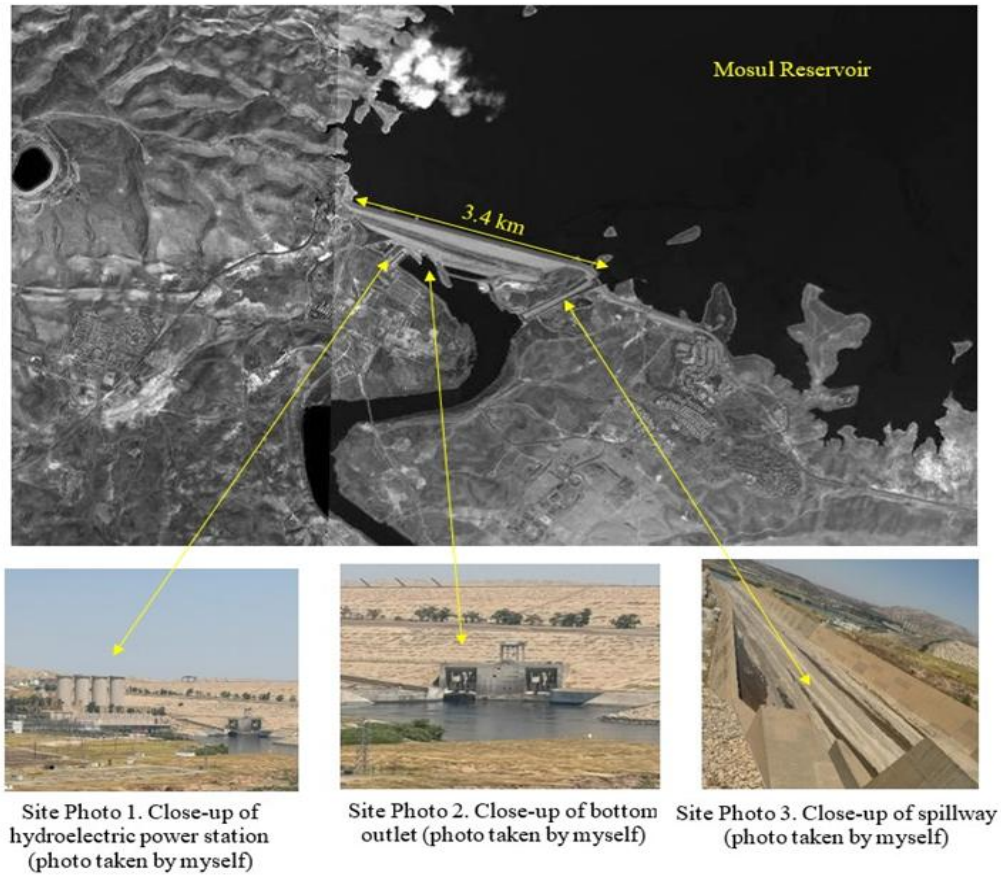

Figure 2. Mosul dam location over land on the SAR intensity image and some site photos of the dam parts

3. Datasets

3.1. Field survey data

In this study, the results of the periodic monitoring of Mosul Dam were obtained by an engineering team assigned to this task and affiliated with the General Survey Authority in Iraq. This team conducts regular and continuous field surveys using high-precision traditional surveying instruments. The collected data, which was obtained with considerable effort, is crucial for monitoring the dam's stability. It consists of elevation measurements for fixed points on the dam's structure (benchmarks), as illustrated in Figure 3, which shows their distribution. These field surveys were conducted on the dates specified in Table 1.

Table 1. Date details of field survey

Field visit number	Date
1	November-2013
2	March-2016
3	December-2016
4	August-2017
5	February-2018
6	September-2018
7	March-2019
8	December-2019
9	September-2020
10	September -2021
11	July-2022
12	December -2022
13	July -2023
14	December -2023
15	may-2024
16	December -2024

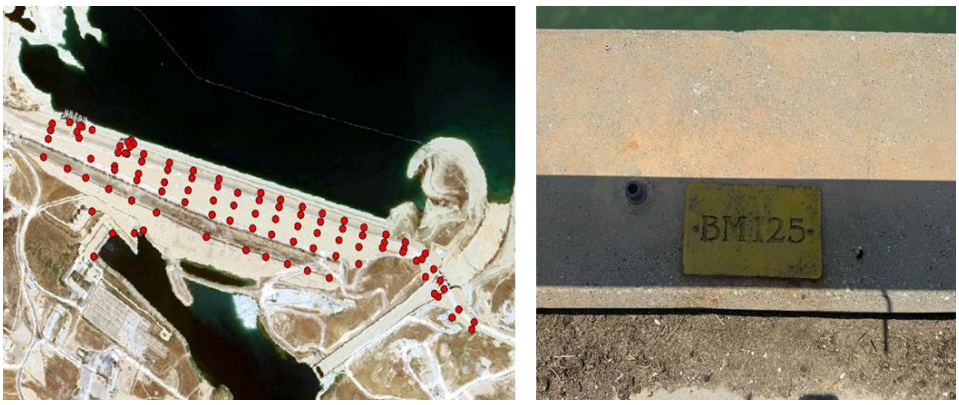

Figure 3. Distribution of fixed points (BM) on the dam body

3.2. SAR data

The second type of data includes ascending imagery from the ALOS-2 and Sentinel-1 satellites, along with Digital Elevation Model (DEM) data, which were utilized for SBAS-InSAR processing. Sentinel-1 satellite images were provided by the European Space Agency. It was launched in October 2014. The ALOS-2 satellite images were provided by the Japan Aerospace Exploration Agency (JAXA) and launched in May 2014.

The DEM used in the research was obtained by the Shuttle Radar Topography Mission (SRTM) sensor, with a spatial resolution of 30 m. Sentinel-1 is a C-band radar satellite with a wavelength of about 5.6 cm, which has certain limitations in densely vegetated areas. It can penetrate clouds and is not affected by weather and climate. It can be used to study the change in flood areas, landslides, and forest fire monitoring, and so on, and the data type is

L1.1, slant-distance single look complex (SLC) mode. The time span is from 15 November 2015 to 25 April 2024, with a total of 117 images, The imaging mode is interferometric wide (IW) swath, the polarization mode is VV, the average incident angle is 33.91, and the ground resolution is 5 20 m. ALOS-2 is the only L- and SAR satellite in operation, with a wavelength of about 23.5 cm and a frequency of 1.2 GHz. The ALOS-2 satellite can obtain observation data without the influence of climate conditions, and time and the type of the data is L1.1. The time span is from 23 November 2014 to 17 March 2024, with a total of 21 images. The resolution is 10 m and the incident angle is 36.28, the polarization mode is HH. Detailed information on the two satellites data is provided in Table 2.

Table 2. Details specification and image view of ALOS-2 and Sentinel-1 images

Feature	Sentinel-1	ALOS-2
Orbital direction	Ascending	Ascending
Temporal coverage	15 November 2015 to 25 April 2024	23 November 2014 to 17 March 2024
Level	L1.1	L1.1
Polarization	VV	HH

Combining Sentinel-1 and ALOS-2 satellite data for ground deformation analysis provides a synergistic advantage by leveraging the unique strengths of both radar systems as shown in the table 3.

Table 3. Comparative Advantages of Sentinel-1 and ALOS-2 SAR Data for Integrated Ground Deformation Monitoring

No.	aspect	Sentinel-1 (C-band)	ALOS-2 (L-band)	Benefit of combination
1	Radar Wavelength	Shorter wavelength (~5.6 cm); sensitive to surface changes	Longer wavelength (~23.6 cm); penetrates vegetation	The combination allows for more complete coverage of different land surfaces. Sentinel-1 detects fine-scale, surface-level shifts, while ALOS-2 captures deeper, longer-term ground motion even in dense vegetation or soft soils.
2	Temporal Resolution	High revisit frequency (6–12 days)	Moderate revisit interval (14–46 days)	Merging the two allows for a balance between frequency and consistency, ensuring high temporal coverage (Sentinel-1) without sacrificing coherence or quality over challenging terrains (ALOS-2).
3	Coherence Retention	Lower in vegetated/low-backscatter areas	High in vegetated and rural regions	Balanced quality and consistency over varied terrain
4	Surface vs. Subsurface Detection	Best for surface-level movements (e.g., dam crest)	Effective for deeper/subsurface movement	Comprehensive assessment of structural and foundational changes
5	Validation and Accuracy	Needs validation in low-coherence areas	Enables robust validation via coherence	Cross-verification enhances result reliability
6	Operational Redundancy	Open-access and frequently updated	Commercial, provides additional resilience	Ensures monitoring continuity and data reliability
7	Nonlinear Deformation Detection	Detects short-term or transient events	Captures long-term, non-linear deformations	Enables better characterization of deformation dynamics

4. Methodology and Processing

4.1. Field survey analysis

Ongoing field surveys for Mosul Dam are subject to an organized control of quality, to obtain accurate and reliable information. These procedures commence with the production of a survey plan, involving routine checking of benchmarks on the dam body and foundations,

and a time-based measurement regime related to the filling and drawdown of reservoirs. Total stations and geodetic GPS instruments are employed for the surveys, and these instruments are regularly calibrated in accordance with the manufacturers' recommendations. Field personnel undergoes training on standardized recording methods to ensure uniformity of procedures. Replicate measurements at the same positions are important to confirm the consistency of results and identify possible deviations with the help of a quick review of data on-site (field checks) and the remeasurements, if needed. Correction methods, such as the differential GPS unfoldments, correction of atmospheric pressure and temperature, are used to eliminate the environmental disturbances. Following the survey, the survey data is analyzed using engineering and analytical programs to determine if the responses retrieved in the new measurements are consistent with earlier measurements and to insight anomalies. Procedures and results for all activities are reported in semiannual technical reports with tables and figures. In some sensitive cases, the data are reviewed by third parties or international experts like the U.S. Army Corps of Engineers (USACE). This integrated approach upgrades the accuracy of field measurements, ensuring precise technical evaluation of the dam's condition and structural safety.

This accurate field data was obtained in the form of 32 Excel files, which were systematically filtered, processed, and analyzed to extract historical displacement and velocity. The data processing involved organizing and applying statistical techniques to ensure accuracy. Vertical displacement is determined by taking the difference in elevation between two time points at the same location, a negative value indicates subsidence, while a positive value indicates uplift. The velocity is then calculated by dividing the vertical displacement by the corresponding time interval. Various mathematical functions and tools were used to compute trends, averages, and deviations. Graphs and charts were generated to visualize displacement patterns over time. The analysis provided insights into velocity fluctuations and historical displacement trends. These findings contribute to a better understanding of the dam displacement behavior.

$$\text{Vertical Displacement} = \text{Elevation (later)} - \text{Elevation (earlier)}$$
$$\text{Velocity} = \text{Vertical Displacement} / \text{Time Interval} \quad (1)$$

4.2. SBAS processing

SBAS, initially introduced by Berardino et al. (2002), involves a two-step processing approach that utilizes multiple unwrapped Differential InSAR interferograms. This method effectively combines all SB interferograms, making it particularly suitable for areas with fewer stable reflectors, such as rural or natural landscapes. The algorithm incorporates an estimation of topographic errors to enhance its robustness. Additionally, the high spatial density of the imaged pixels enables atmospheric phase artifact filtering on the computed space–time deformation measurements, a process comparable to the PSI technique. SBAS enables the generation of deformation time series and average velocity maps by solving a system of interferometric phase equations under the assumption of a linear or nonlinear displacement model. The technique is particularly valuable for studying slow-moving deformation phenomena such as subsidence, landslides, and tectonic motion.

For the monitoring of the Mosul Dam, the SBAS-InSAR approach has been chosen, since it is very well suited for the complex geographical/ geological characteristics of the investigated site. The dam is surrounded by rural region dominated by a seasonal vegetation cover as well as karstic topography, where other InSAR processing methods such as PS-InSAR that depend on the existence of buildings or permanent radar reflectors (e.g., urban structures) would not work as well. Furthermore, the SBAS supports L-band radar imagery from satellites like ALOS-2, with deep vegetation penetration and higher coherence in rural zones, which improve the accuracy of the output. Thus, the properties of SBAS are highly

appropriate to the distinct constraints of the Mosul Dam site, such as soil, land cover, and temporal behavior of deformation.

The general form of the SBAS phase equation is:

$$\varphi_{i,j=}\Delta\varphi_{i,j}^{disp} + \Delta\varphi_{i,j}^{topo} + \Delta\varphi_{i,j}^{atm} + \Delta\varphi_{i,j}^{noise} \quad (1)$$

Where:

$\varphi_{i,j}$ is the interferometric phase between acquisitions i and j,

$\Delta\varphi_{i,j}^{disp}$ is the phase due to ground displacement,

$\Delta\varphi_{i,j}^{topo}$ is the residual topographic phase,

$\Delta\varphi_{i,j}^{atm}$ is the atmospheric phase delay, and

$\Delta\varphi_{i,j}^{noise}$ includes decorrelation and other noise contributions (Lanari et al., 2007).

This study utilized the SBAS method to perform interferometric analysis on data from Sentinel-1 and ALOS/PALSAR-2 sensors. The steps taken to calculate the displacement rates affecting the study area are illustrated in Figure 4.

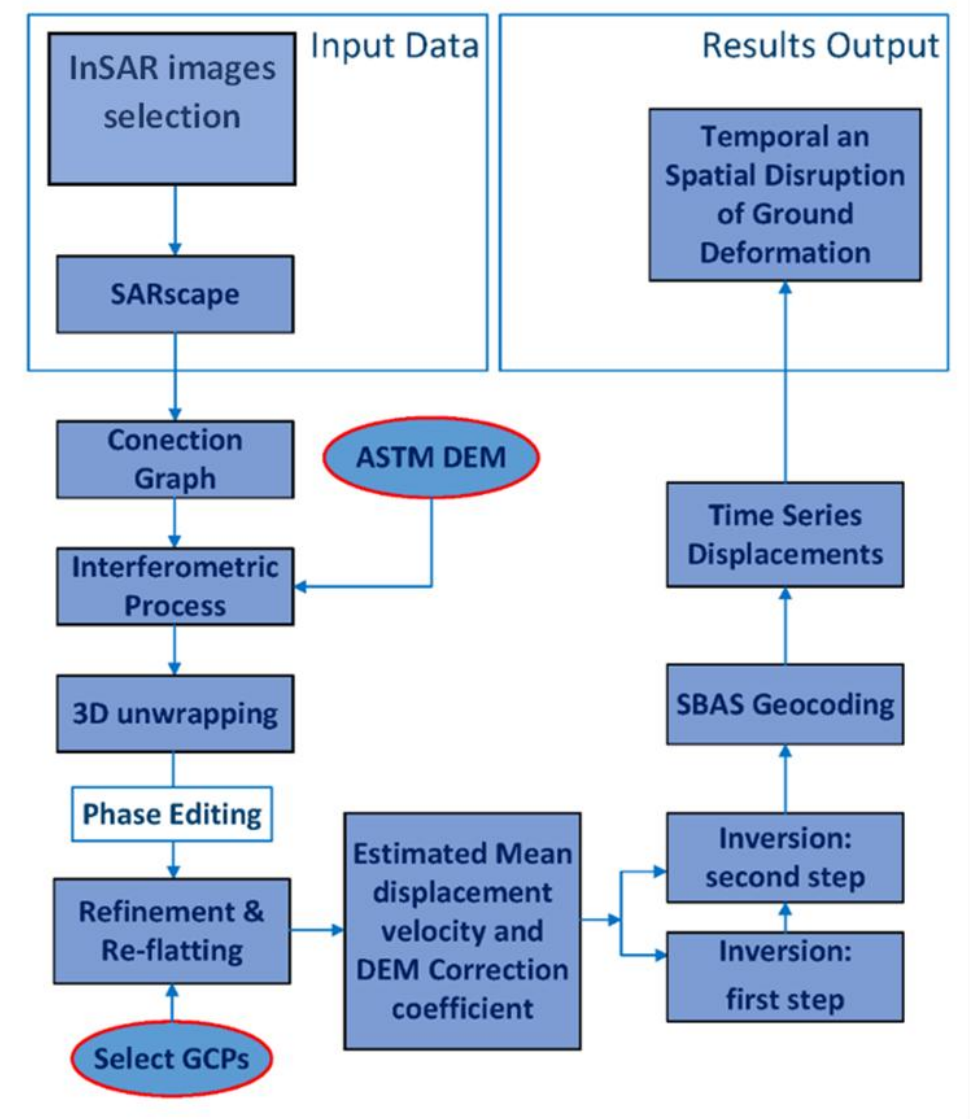

Figure 4. SBAS-InSAR technology flow chart

To regulate the number of interferometric pairs generated, thresholds for the time baseline and spatial baseline were applied, according to the interval of SAR data. in order to ensure the coherence of the data, (the time baseline of Sentinel-1 data were set to 180 days while the spatial baseline were set to 45% of the maximum baseline distance, and 472 interferometric pairs were obtained and the time baseline of ALOS-2 data were set to 1500

days while the spatial baseline were set to 50% of the maximum baseline distance, and 156 interferometric pairs were obtained), used for estimating surface deformation parameters. The baseline connection diagrams are shown in Figure 5a, b, respectively.

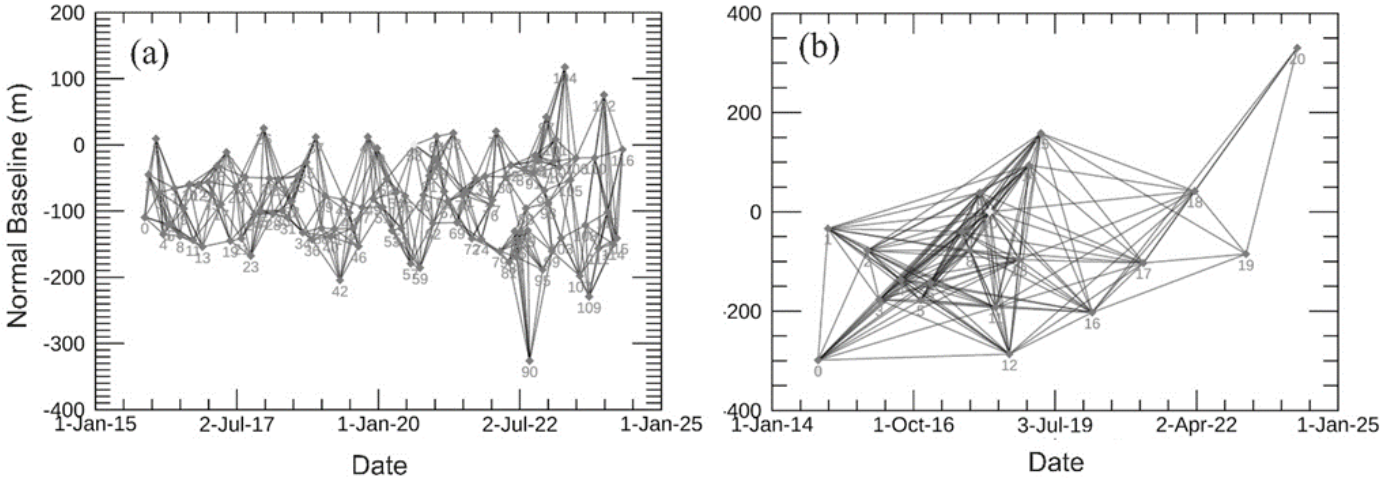

Figure 5. (a) Spatial and temporal baseline of SBAS pairs of Sentinel-1 images; (b) Spatial and temporal baseline of SBAS pairs of ALOS-2 images

The threshold values used in processing Sentinel-1 and ALOS-2 data—such as temporal coherence thresholds, maximum spatial and temporal baselines were determined based on a combination of previous studies, default settings recommended by specialized software (e.g., SARscape). These values aim to achieve an optimal balance between data quality and point density, particularly in a geologically complex and partially vegetated region like the Mosul Dam. For instance, the temporal coherence threshold was calibrated to exclude low-quality pixels while preserving meaningful deformation signals. This methodology enhances the scientific transparency and accuracy of the processing workflow.

5. Results

Figure 6a, b and c present he classification of displacement velocity based on three methodologies: field survey data analysis, SBAS Sentinel-1 and ALOS-2 data analysis. The average velocity of the dam, as determined by the field survey, was -2.82 mm/year, while the SBAS Sentinel-1 and ALOS-2 results indicated an average vertical velocity of -2.31, -2.98 mm/year respectively. The red points in Figure 6 highlight areas where the subsidence velocity exceeds 5 mm/year. Notably, in the three study cases, these critical points are concentrated in the central region of the dam, which exhibited the highest subsidence rates. Specifically, the average vertical velocity in this region reached -6.76 mm/year according to the field survey and -6.21, -5.82 mm/year based on SBAS Sentinel-1 and ALOS-2 results respectively. Both methodologies consistently identified the central portion of the dam as the most vulnerable to subsidence. This observation aligns with expectations, as this region corresponds to the old riverbed prior to the dam's construction, rendering it structurally weaker compared to other foundation areas. In this study, the base year for subsidence measurements was set at 2013 for field survey data and 2.15, 2014 for SBAS Sentinel-1 and ALOS-2 results. The analysis revealed temporal variations in displacement values, fluctuating between uplift and subsidence over the years. These fluctuations can be attributed to multiple factors, including variations in the water level of the reservoir and heterogeneity in the geomechanical properties of the dam foundation. The field survey recorded a maximum uplift of 13.31 mm in 2024, alongside a peak subsidence of 103.5 mm in the same year. In comparison, the Sentinel-1 processing results indicated the highest uplift of 33.22 mm in 2018 and the greatest subsidence of 74.40 mm in 2024. Similarly, the SBAS ALOS-2 processing results showed the maximum uplift of 33 mm in 2017 and the most pronounced subsidence of 51.7 mm in 2024.

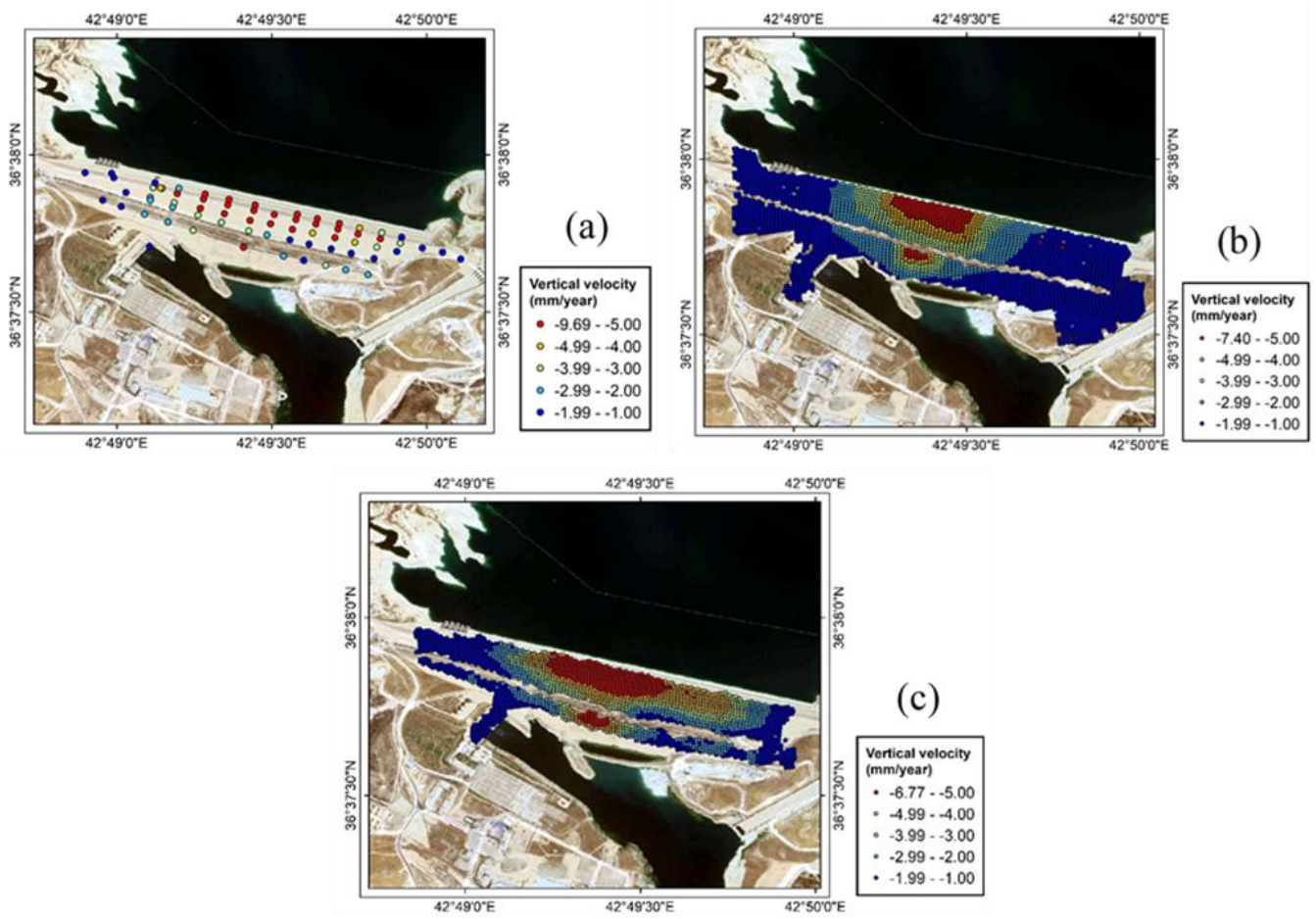

Figure 6. Spatial distribution of vertical velocity in Mosul Dam (a) Calculated from field survey analysis; (b) Calculated from SBAS Sentinel-1 Data; (c) Calculated from SBAS ALOS-2 Data. The base map is taken from google earth

To clarify the distribution of displacement velocities for the three datasets of study the Figure 7 which is three histograms (labeled a, b, and c) indicates All three datasets show negative mean displacement velocities—ranging from -2.31 mm/year in (b) to -2.98 mm/year in (c)—indicating overall land subsidence across the datasets. Histogram (a), with a mean of -2.82 mm/year, reveals a right-skewed distribution with a pronounced concentration of values between -1.2 and -0.6 mm/year. In contrast, histogram (b) exhibits a sharper peak near -1.9 mm/year and a large sample size, with frequencies exceeding 500, suggesting a widespread, consistent rate of subsidence across a larger area. Histogram (c) displays a bimodal distribution with significant variability, implying localized zones with differing rates of movement. The comparative analysis suggests a marked heterogeneity in spatial deformation patterns.

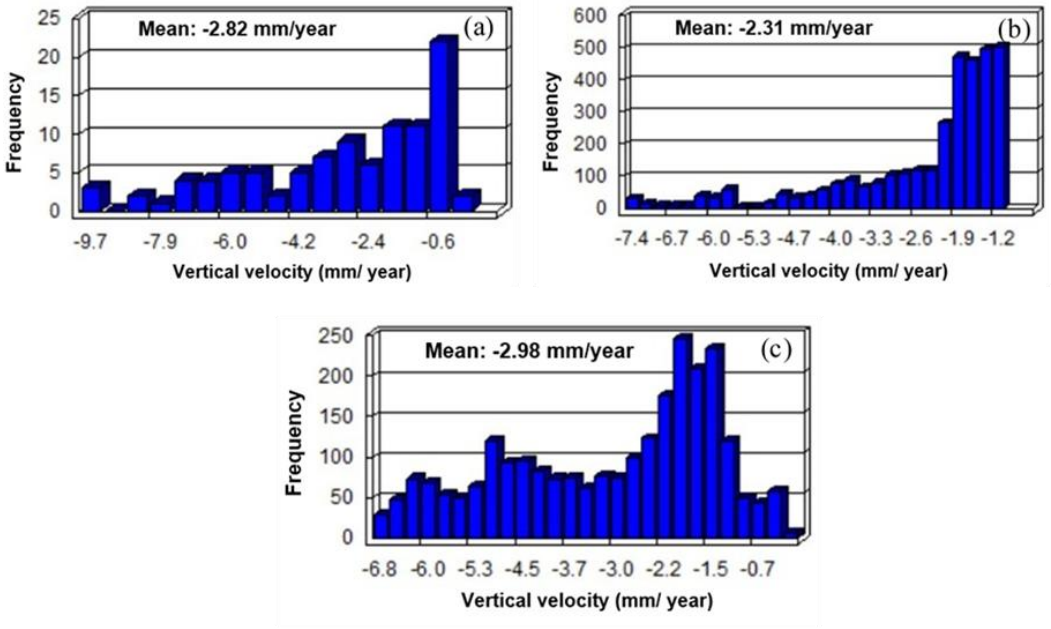

Figure 7. Frequency Distribution of Ground Vertical Velocities Across the three Observational Datasets of study (a) field survey analysis; (b) SBAS Sentinel-1; (c) SBAS ALOS-2

The observed subsidence rates at Mosul Dam which ranged approximately between (-3 to -2 mm/year) across the three study cases SBAS-InSAR on Sentinel-1 and ALOS-2 images, as well as historical field survey measurements (benchmarks) reveal the presence of slow but continuous ground movement, particularly in the mid-dam area, where the geological structure is more fragile (it runs through an ancient riverbed and contains soluble gypsum rocks). According to international standards such as those of the International Commission on Large Dams (ICOLD) and the U.S. Army Corps of Engineers (USACE), we can say that there is no fixed value considered critical for all dams, as the risk assessment depends on the geological context and the type of foundation. In terms of safety, these rates are considered within acceptable limits under normal conditions if they are not accompanied by sudden changes or acceleration of movement. However, their persistence without a geological or engineering explanation or treatment could indicate a growing risk in the medium or long term. On the other hand, the spatial variations in subsidence rates, particularly between the center and edges of the dam, raise the possibility of differential settlement, which could lead to internal stresses in the dam body that affect its structural integrity.

Figure 8 comprises three scatter plots (labeled a, b, and c), each assessing the linear correlation between velocity of ground deformation in Mosul dam measured in (mm/year) obtained from the three study data sources. Plot (a) compares SBAS Senti-nel-1 with SBAS ALOS-2, revealing a relatively strong linear relationship (R^2 = 0.6855) with a regression equation of y = 0.8047x – 0.239. This suggests that Sentinel-1 measurements closely align with those from ALOS-2, albeit with some variability. Plot (b) compares SBAS Sentinel-1 with field survey data, yielding the weakest correlation (R^2 = 0.5281, y = 0.4175x – 1.4647). Finally, plot (c) compares SBAS ALOS-2 with the field survey data and shows the highest degree of correlation (R^2 = 0.7923, y = 0.5847x – 0.9854), reflecting that ALOS-2 more reliably matches the field observations. Despite the general agreement among the three datasets, the correlation between Sentinel-1 SBAS-InSAR and field survey results is notably weaker. This can be attributed to several factors, including the presence of seasonal vegetation and the rural terrain around Mosul Dam, which reduce temporal coherence and increase signal decorrelation in C-band imagery. In contrast, ALOS-2's L-band provides better penetration and coherence, explaining its stronger correlation with field benchmarks. Sentinel-1's higher revisit rate also makes it more sensitive to short-term surface variations—such as rainfall or anthropogenic activity—not captured by periodic field

surveys. Additional sources of discrepancy include differences in spatial alignment between radar pixels and benchmark points, as well as slight variations in geolocation accuracy and sensor calibration. Collectively, these results underscore the relatively superior performance of ALOS-2 over Sentinel-1 in replicating field-measured deformation velocities, suggesting that the longer wavelength L-band SAR (ALOS-2) is less affected by decorrelation in the observed area. This comparative analysis supports the integration of ALOS-2 data for high-fidelity deformation monitoring in complex terrains.

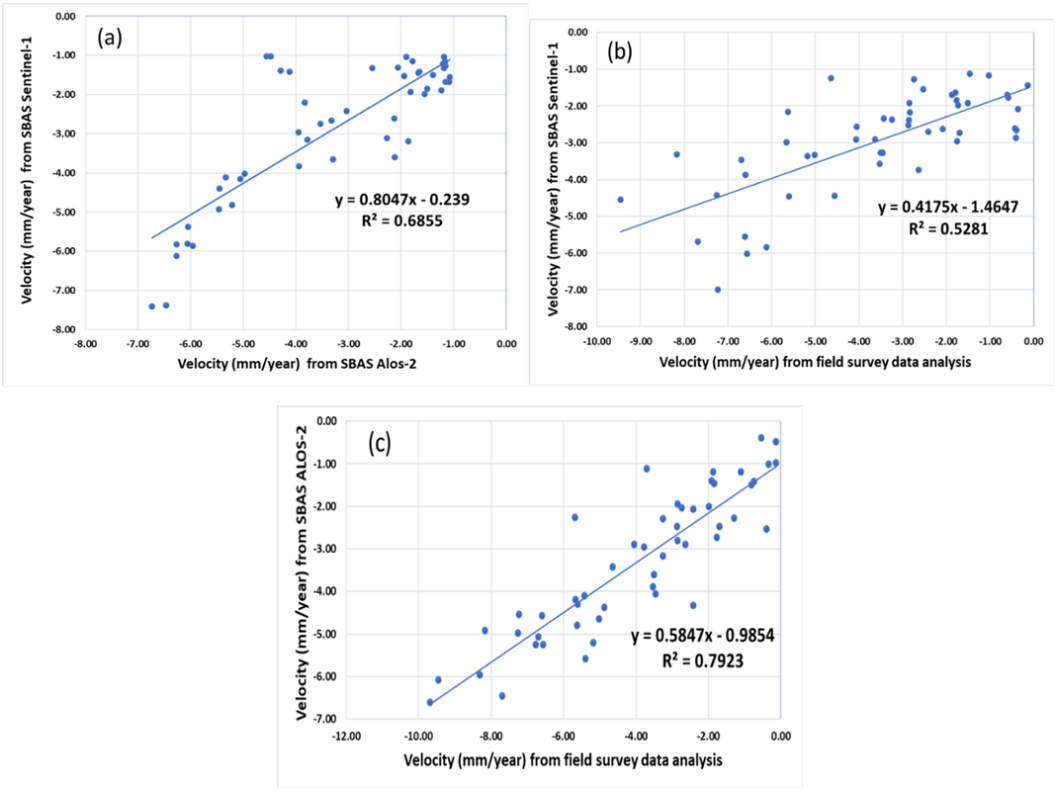

Figure 8. Linear correlation of surface vertical velocity in Mosul Dam (a) SBAS Sentinel-1 versus SBAS ALOS-2; (b) Field survey versus SBAS Sentinel-1; (c) Field survey analysis versus SBAS ALOS-2

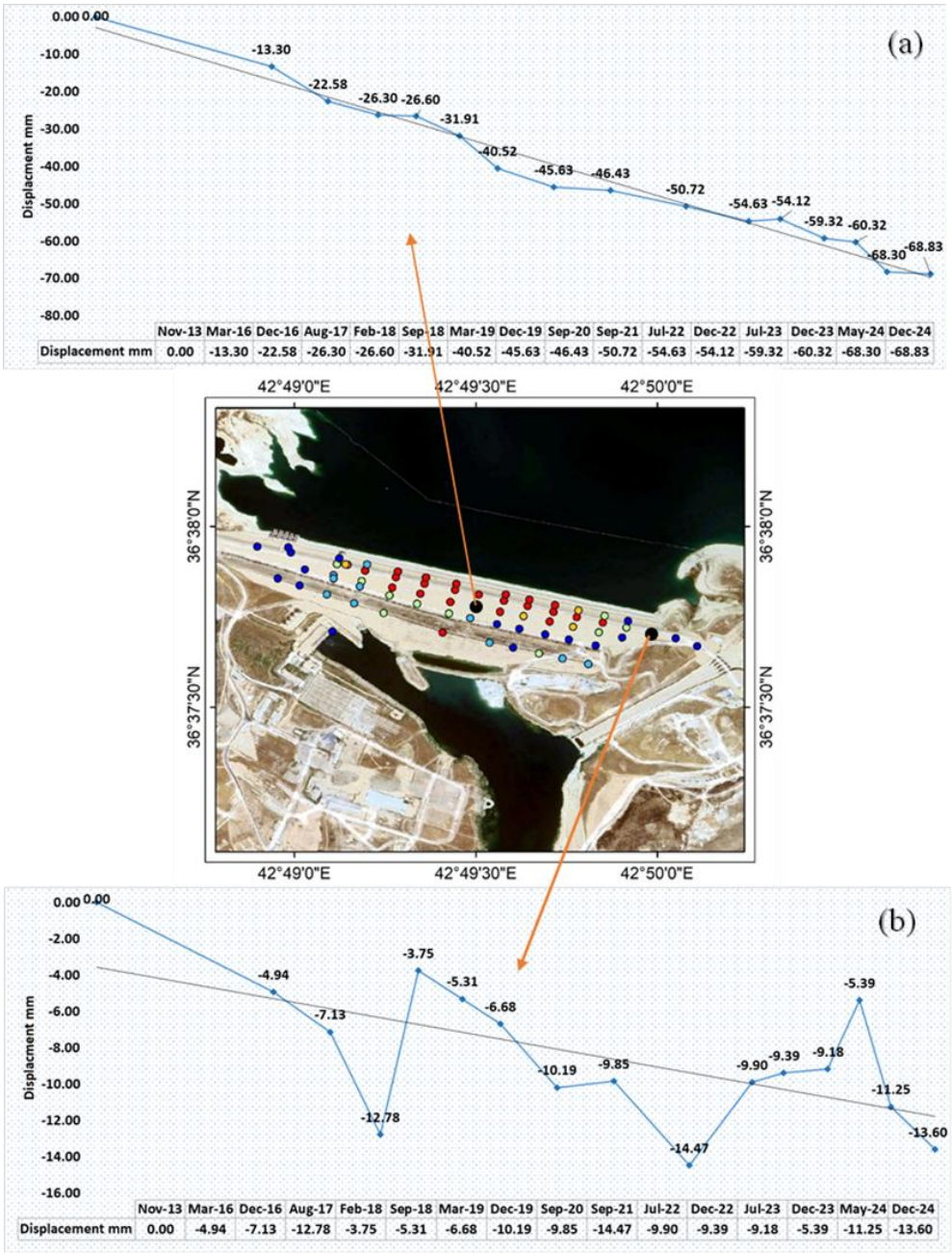

Figure 9. The figure shows the displacement graph based on the results of field survey for two points, one at the center of dam (point a) and the second point at the side of dam (point b). The map represents the spatial distribution of the velocity

To further elucidate the spatial pattern of displacements, two representative points were selected around the dam body for each dataset: point a, located within the red-highlighted central displacement area, and point b, positioned in the marginal segment of the dam, as illustrated in Figure 9, Figure 10 and Figure 11. The results indicated significant differences in subsidence and uplift magnitudes between these points. The time-series analysis revealed that the three study cases agreed that points a followed a relatively consistent linear pattern suggesting continuous settlement in the dam's central region. In contrast, point b exhibited alternating periods of uplift and subsidence, reflecting localized variations in foundation stability on the dam's periphery.

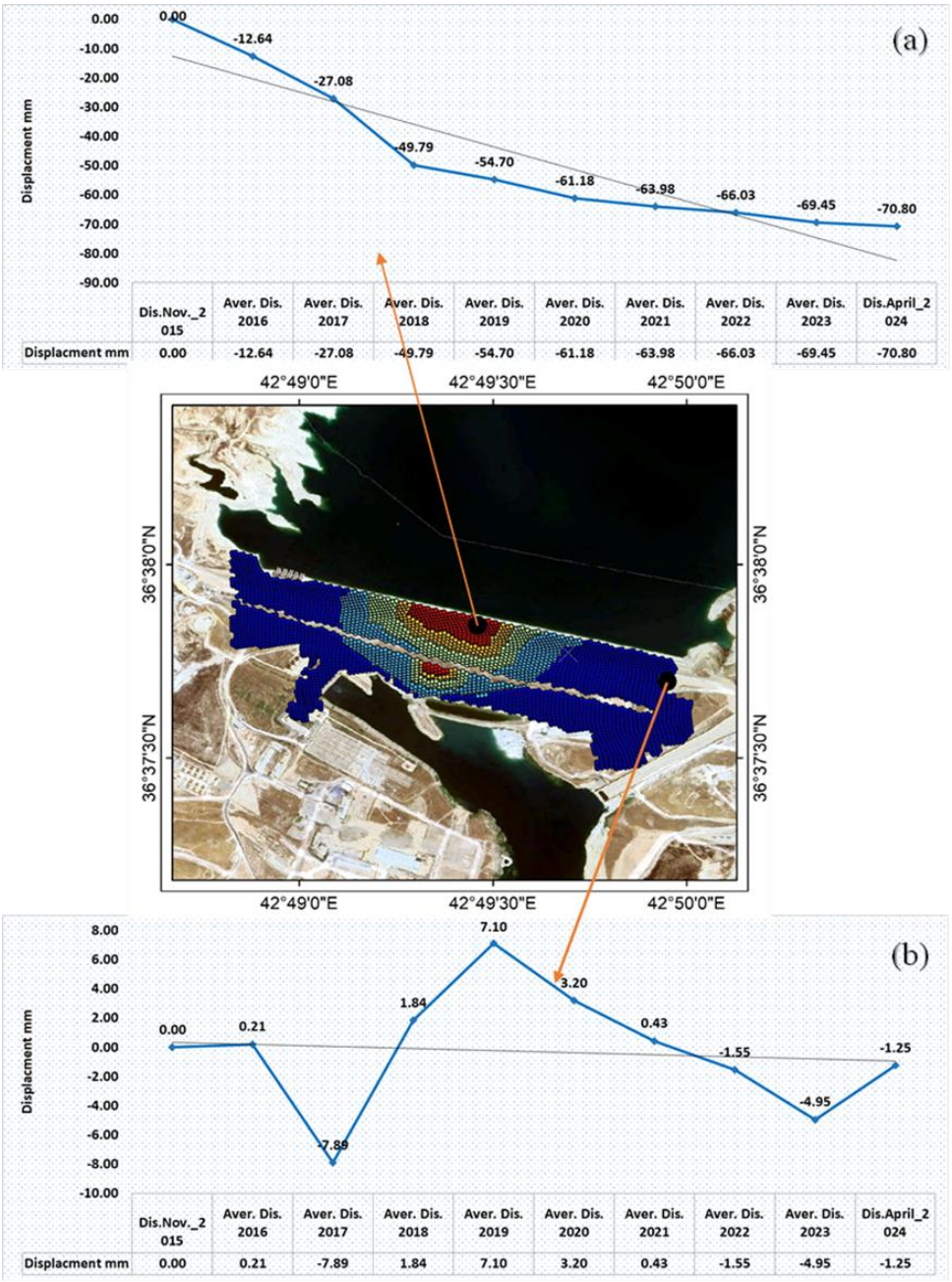

Figure 10. The figure shows the displacement graph based on the results of SBAS Sentinel-1 processing for two points, one at the center of dam (point a) and the second point at the side of dam (point b). The map represents the spatial distribution of the velocity

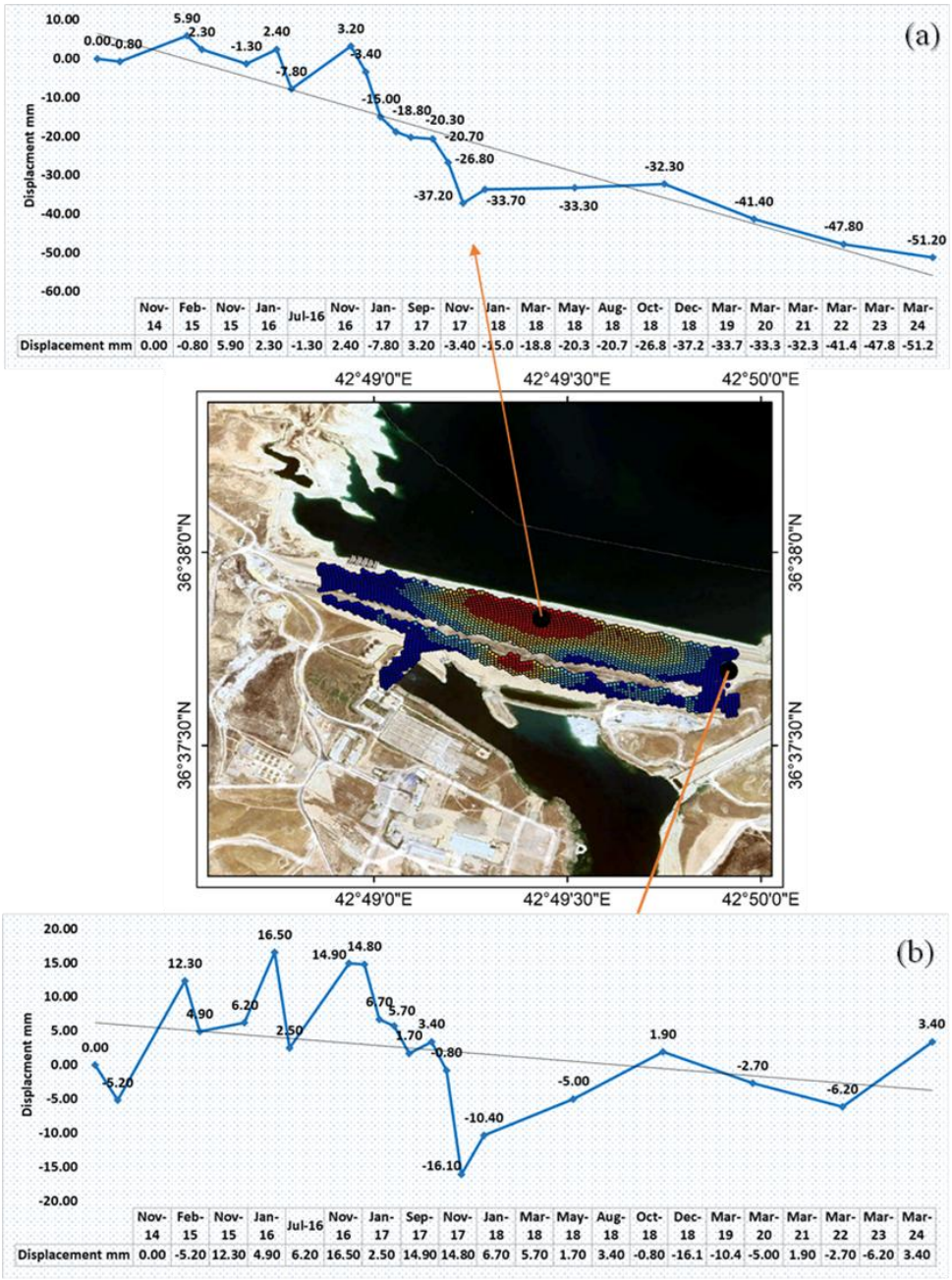

Figure 11. The figure shows the displacement graph based on the results of SBAS ALOS-2 processing for two points, one at the center of dam (point a) and the second point at the side of dam (point b). The map represents the spatial distribution of the velocity

Figures 12 a, b and c depict the spatial classification of cumulative displacement (Sentinel-1) values (in mm) for two distinct study cases in 2024, offering insight into the cumulative displacement trends within the study area. Despite noticeable differences in absolute displacement values between the three methodologies, a strong correlation is evident in the spatial distribution of subsidence. Field survey analysis recorded an average displacement of -28.2 mm, whereas the SBAS Sentinel-1 and ALOS-2 data analysis yielded an average displacement of -15.5, -14.4 mm respectively. A critical observation from these figures is that the central region of the dam exhibits the highest subsidence rates, suggesting a localized concentration of displacement forces. In contrast, the peripheral areas of the dam, while still affected by subsidence, experience significantly lower displacement magnitudes.

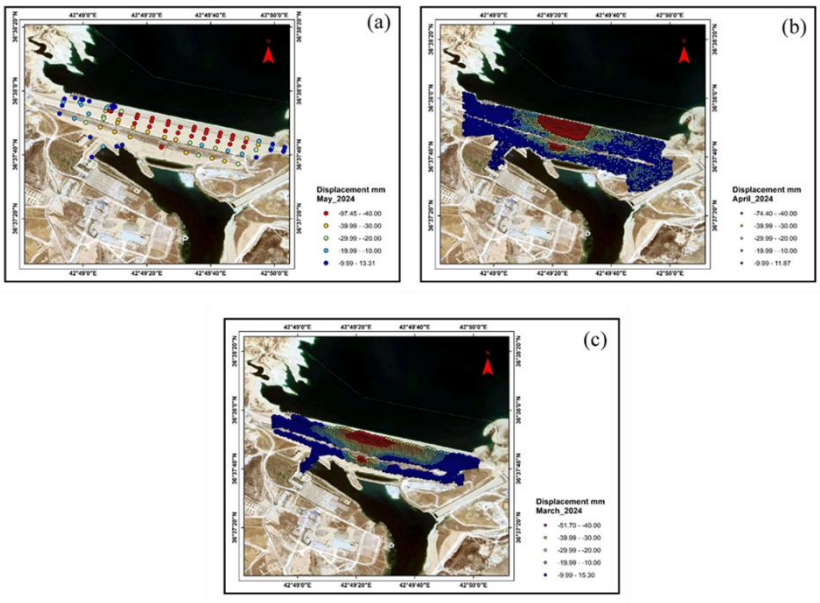

Figure 12. Distribution of cumulative displacement in the year 2024 (a) based on field survey; (b) based on SBAS Sentinel-1 Data; (c) based on SBAS ALOS-2 Data.

6. Discussion

The analysis of displacement velocities derived from field surveys, SBAS Sentinel-1, and ALOS-2 datasets provides a consistent narrative of ongoing ground subsidence at Mosul Dam. All three methodologies identified the central section of the dam as the most deformation-prone area—a finding that corroborates earlier assessments by the U.S. Army Corps of Engineers (USACE, 2006), which highlighted the structural vulnerability of this region due to its foundation over soluble gypsum and the old riverbed. This convergence between historical expert evaluations and satellite-based observations confirms the persistent geotechnical weakness of the dam's midsection and justifies its prioritization for ongoing monitoring and intervention.

Compared to previous InSAR-based studies, such as those by (Milillo et al., 2016), which employed COSMO-SkyMed data to assess deformation at Mosul Dam, the current research provides a broader temporal perspective through the integration of SBAS processing with both L-band (ALOS-2) and C-band (Sentinel-1) datasets. While Milillo et al. (2016) identified localized subsidence zones, their temporal coverage was limited. Our findings expand upon this by offering a longer multi-year deformation time series and confirm the continuation of the deformation trends they identified, also reported a maximum displacement of approximately −14.6 mm/year, identifying accelerated subsidence following the 2014 interruption of grouting operations. In contrast, our study observed more moderate deformation rates averaging between (−2 to -3 mm/year) for all three methodologies of study, suggesting partial stabilization of deformation, this is most likely due to the resumption of maintenance and foundation injection operations

Moreover, this study contributes new comparative insights by directly evaluating the differences between ALOS-2 and Sentinel-1 performance over karst-prone dam foundations—a research gap noted by Li et al. (2023) and Yang et al. (2023), who advocated for deeper analysis of SAR wavelength effects in heterogeneous geological environments. The stronger correlation between ALOS-2 and field survey data observed here supports previous findings that L-band sensors offer superior coherence in vegetated and rural regions (Rosenqvist et al., 2007), and confirms the recommendation by Zhou et al. (2016) to use L-band SBAS for long-term deformation monitoring in soft and soluble terrain.

In addition, while previous dam monitoring studies (Mazzanti et al., 2015; Tomás et al., 2013) have validated the efficacy of SBAS-InSAR in detecting slow deformation, few have applied this technique to a dam with such complex geomechanical conditions as Mosul.

Unlike prior works, we included histogram distributions and time-series analyses of representative benchmarks, revealing subsidence asymmetry between the dam center and edges an observation consistent with Emadali et al. (2017) documentation of non-linear deformations in earth dams.

By integrating SBAS-InSAR with long-term field data, this study validates InSAR-derived velocities and offers novel insights into the spatial and temporal evolution of deformation at a high-risk dam. As one of the first regional studies to combine multi-sensor SAR data with decades-long field observations, it significantly advances dam safety monitoring frameworks in data-limited regions like Iraq.

7. Conclusions

This study investigates land subsidence at the Mosul Dam using two distinct types of data, the first dataset comprises historical survey measurements collected periodically by the General Authority of Survey in Iraq, the second consists of radar imagery from Sentinel-1 (C-band) and ALOS-2 PALSAR-2 (L-band), processed using Small Baseline Subset Interferometric Synthetic Aperture Radar (SBAS-InSAR) technology. The analysis yielded the following results: based on the field survey data, ground displacement values range from −9.69 mm/year to 0.20 mm/year. The SBAS analysis of Sentinel-1 imagery indicated displacement values between −7.40 mm/year and 0.12 mm/year. Similarly, SBAS analysis of ALOS-2 PALSAR-2 data revealed displacement values ranging from −6.77 mm/year to 0.03 mm/year. The three studies agreed on two important points that represent the essence of the study, the first is that the area in the middle of the dam is the area most exposed to subsidence, this is also considered an examination of the results of the SPAS analysis and a demonstration of its accuracy. The second is the difference in the displacement pattern (uplift and subsidence) between the area in the middle of the dam and the areas on the side of the dam.

This study introduces several important advancements to the current understanding of dam deformation monitoring, particularly for complex geotechnical structures like Mosul Dam. By integrating SBAS-InSAR analysis from both Sentinel-1 (C-band) and ALOS-2 (L-band) satellites with long-term field survey data collected by the General Authority for Survey in Iraq, the research offers a rare and robust validation framework that enhances confidence in satellite-derived deformation trends. Unlike earlier studies that relied on a single data source or had limited temporal coverage, this work provides a multi-year time series that captures consistent subsidence patterns, especially in the structurally vulnerable central zone of the dam built over soluble gypsum and old riverbed deposits. The comparative evaluation between L- and C-band sensors reveals that ALOS-2's L-band data delivers superior coherence and reliability in rural, vegetated, and karst-prone environments an insight that strengthens prior theoretical suggestions with applied evidence. In doing so, it fills a regional research gap by presenting one of the few InSAR-based dam monitoring case studies in Iraq supported by extensive ground truth data. This integrated approach serves as a model for future research and monitoring programs on embankment dams situated in geologically sensitive areas.

Based on the quantitative results obtained from the study using all three measurement techniques (SBAS-InSAR using Sentinel-1 and ALOS-2, and field surveys), there are persistent subsidence rates, with the highest values in the center of the dam. Also based on previous studies confirming the fragility of the foundations, especially the center of the dam, and according to the technical standards followed by organizations such as the International Commission on Large Dams (ICOLD), The study recommends that if the subsidence exceeds the amounts recorded in the study, especially in critical areas (such as the dam center or structural joints), it should be considered a warning sign, especially if accompanied by cracks or leaks. Continued subsidence without stability, or the appearance of an acceleration in the time rate, may require a re-evaluation of the injection plan, or enhanced continuous and strict monitoring.

Future research should expand time series to capture long-term seasonal and hydrological deformation cycles. Incorporating additional geotechnical and hydrological parameters (e.g., pore pressure, reservoir levels, grouting data) to improve interpretation. Applying hybrid InSAR models that combine SBAS and PS-InSAR techniques for enhanced spatial resolution. Investigating the integration of AI-based anomaly detection with InSAR data for real-time risk forecasting. By filling a significant gap in regional dam monitoring studies and offering transferable methodologies, this research supports the development of comprehensive, multi-sensor frameworks for structural health monitoring in critical water infrastructure worldwide.

Acknowledgments: The authors would like to express our gratitude to Prof. Masashi Matsuoka for providing the ALOS-2 PALSAR-2 data free of charge and for all his support.

Author Contributions:

A. A. Azeez: Methodology, Software, Formal analysis, Writing—original, Draft and visualization.

S. Karimzadeh: Methodology, Conceptualization, Data collection, Concept development, Writing—review and editing, Supervision.

K. V. Kamran: Conceptualization, Writing—review and editing, Grammar checking.

M. Matsuoka: Conceptualization, Data collection, Writing—review and editing.

Research and publication ethics statement: In the study, the author/s declare that there is no violation of research and publication ethics and that the study does not require ethics committee approval.

Conflicts of Interest: Khalil Valizadeh Kamran and Sadra Karimzadeh, two co-authors of this manuscript, are members of the journal's Editorial Board. All editorial handling and decisions were made independently, without their involvement. Apart from this, the authors declare no conflict of interest.

References

Al-Ansari, N. (2013). Management of water resources in Iraq: Perspectives and prognoses. *Engineering*, 5(8), 667–68. https://doi.org/10.4236/eng.2013.58080

Al-Ansari, N., & Adamo, N. (2016). Mosul Dam full story: Safety evaluations of Mosul Dam. *Journal of Earth Sciences and Geotechnical Engineering*, 6(3), 185-212.

Al-Ansari, N., Adamo, N., Al-Hamdani, M., Sahar, K., Al-Naemi, R. (2021). Mosul Dam problem and stability. *Engineering*, 13(3), 105-124. https://doi.org/10.4236/eng.2021.133009

Al-Ansari, N., Adamo, N., Knutsson, S., Laue, J., & Sissakian, V. (2020). Mosul Dam: Is it the most dangerous dam in the world? *Geotechnical and Geological Engineering*, 38(3), 5179–5199. https://doi.org/10.1007/s10706-020-01355-w

ASDO. (2023). Association of State Dam Safety, Dams 101. Retrieved May 4, 2025, from https://damsafety.org/dams101

Barone, A., Fedi, M., Pepe, A., Mastro, P., Tizzani, P., & Castaldo R. (2025). Inferring 3D displacement time series through InSAR measurements and potential field theory in volcanic areas. *Scientific Reports*, 15, 4719. https://doi.org/10.1038/s41598-025-88006-3

Berardino, P., Fornaro, G., Lanari, R., & Sansosti, E. (2002) A new algorithm for surface deformation monitoring based on small baseline differential SAR interferograms. *IEEE Transactions on Geoscience and Remote Sensing*, 40(11), 2375–2383. https://doi.org/10.1109/TGRS.2002.803792

Bowen, S. (2007). Office of the special inspector general for Iraq reconstruction. Relief and reconstruction funded work at Mosul dam Mosul, Iraq. Retrieved May 4, 2025, from http://cybercemetery.unt.edu/archive/sigir/20131001121159/http:/www.sigir.mil/files/assessments/PA-07-105.pdf

Brunson, B., Hu, B., & Wang, J. (2020). Synthetic aperture radar phase unwrapping using region-growing with polynomial-based phase prediction. *Geomatica*, 74(4), 196-219. https://doi.org/10.1139/geomat-2020-0013

Cigna, F., & Tapete, D. (2021). Cigna, F., & Tapete, D. (2021). Present-day land subsidence rates, surface faulting hazard and risk in Mexico City with 2014–2020 Sentinel-1 IW InSAR. *Remote Sensing of Environment*, 253, 112161. https://doi.org/10.1016/j.rse.2020.112161

Emadali, L., Motagh, M., & Haghighi, M.H. (2017). Characterizing post-construction settlement of the Masjed-Soleyman embankment dam, Southwest Iran, using TerraSAR-X SpotLight radar imagery. *Engineering Structures*, 143, 261–273. https://doi.org/10.1016/j.engstruct.2017.04.009

Ferretti, A. Prati, C. & Rocca, F. (2000). Permanent scatterers in SAR interferometry. *IEEE Trans, Geosci. Remote Sensing*, 39(1), 8–20. https://doi.org/10.1109/36.898661

Gabriel, A., Goldstein, R., & Zebker, H. (1989). Mapping small elevation changes over large areas: Differential Radar interferometry. *Journal of geophysical Research*, 94(7), 9183–9191. https://doi.org/10.1029/JB094iB07p09183

Gama, F., Mura, J., Paradella, W., & de Oliveira, C. (2019). Advanced DInSAR analysis on dam stability monitoring: A case study in the Germano mining complex (Mariana, Brazil) with SBAS and PSI techniques. *Remote Sensing Applications: Society and Environment*, 16, 100267. https://doi.org/10.1016/j.rsase.2019.100267

Gheorghe, M., & Arma¸ S. I. (2016). Comparison of multi-temporal differential interferometry techniques applied to the measurement of Bucharest city subsidence. *Procedia Environ, Sci*, 32, 221–229. https://doi.org/10.1016/j.proenv.2016.03.027

Gracon LLC. (2023). Advantages of dams, benefits & importance of dam construction. Retrieved May 4, 2025, from https://graconllc.com/advantages-of-dams

Karimzadeh, S., Zulfikar, A. C., & Matsuoka, M. (2024). Time series analysis of L-band PALSAR-2 images in Istanbul and Kocaeli, Turkey. *Big Earth Data*, 8(3), 467-493. https://doi.org/10.1080/20964471.2024.2320466

Khafaji, K., & Ben Hamed, B. (2025). Improving the prediction of evaporation variable in Mosul Dam using ARIMA model and time series analysis. Fusion: *Practice and Applications (FPA)*, 17(02), 342-355.

Lanari, R., Casu, F., Manzo, M., Zwni, G., Berardino, P., Manunta, M., & Pepe, A. (2007). An overview of the small baseline subset algorithm: a DInSAR technique for surface deformation analysis. *Pure and applied geophysics*, 164(4), 637–661. https://doi.org/10.1007/978-3-7643-8417-3_2

Li, W., Wu, Y., Gao, X., Wang, W., Yang, Z., & Liu, H. (2023). The distribution pattern of ground movement and co-seismic landslides: A case study of the 5 September 2022 Luding earthquake, China. *Journal of Geophysical Research: Earth Surface*, 129(5). https://doi.org/10.1029/2023JF007534

Martire, D., Iglesias, R., Monells, D., Centolanza, G., Sica, S., Ramondini, M., Pagano, L., Mallorquí, J., & Calcaterra, D. (2014). Comparison between differential SAR interferometry and ground measurements data in the displacement monitoring of the earth-dam of Conza della Campania (Italy). *Remote sensing of environment*, 148, 58–69. https://doi.org/10.1016/j.rse.2014.03.014

Mazzanti, P., Perissin, D., & Rocca, A. (2015). Structural health monitoring of dams by advanced satellite SAR interferometry: investigation of past processes and future monitoring perspectives. Proceedings Book of 7th International Conference on Structural Health Monitoring of Intelligent Infrastructure, Torino, Italy.

Milillo, P., Bürgmann, R., Lundgren, P., Salzer, J., Perissin, D., Fielding, E., Biondi, F., & Milillo, G. (2016). Space geodetic monitoring of engineered structures: The ongoing destabilization of the Mosul Dam, Iraq. *Scientific Reports*, 6, 37408. https://doi.org/10.1038/srep37408

Milillo, P., Perissin, D., Salzer, J., Lundgren, P., Lacava, G., Milillo, G., & Serio, C. (2016). Monitoring dam structural health from space: Insights from novelInSAR techniques and multi-parametric modeling applied to the Pertusillo dam Basilicata, Italy. *International Journal of Applied Earth Observation and Geoinformation*, 52, 221–229. https://doi.org/10.1016/j.jag.2016.06.013

Othman, A., Al-Maamar, A., Al-Manmi, D., Liesenberg, V., Hasan, S., Al-Saady, Y., Shihab, A., & Khwedim, K. (2019). Application of DInSAR-PSI technology for deformation monitoring of the Mosul Dam, Iraq. *Remote Sensing*, 11(22), 2632. https://doi.org/10.3390/rs11222632

Roque, D., Perissin, D., Falcão, A. P., Fonseca, A. M., Henriques, M. J., & Franco, J. (2015). Dams regional safety warning using time-series InSAR techniques. Proceedings Book of Second International Dam World Conference, Lisbon, Portugal, 21–24.

Rosenqvist, A., Shimada, M., Ito, N.,&Watanabe, M. (2007). ALOS PALSAR: A pathfinder mission for global-scale monitoring of the environment. *IEEE Transactions on Geoscience and Remote Sensing*, 45(11), 3307–3316. https://doi.org/10.1109/TGRS.2007.901027

Sica, S., & Pagano, L. (2009). Performance-based analysis of earth dams: Procedures and application to a sample case. *Soils and Foundations*, 49(6), 921–940. https://doi.org/10.3208/sandf.49.921

Tomás, R., Cano, M., Garcia-Barba, J., Vicente, F., Herrera, G., Lopez-Sanchez, J. M., & Mallorquí J. J. (2013). Monitoring an earthfill dam using differential SARinterferometry: La Pedrera Dam, Alicante, Spain. *Engineering Geology*, 157, 21–32. https://doi.org/10.1016/j.enggeo.2013.01.022

Wang, P., Xing, C., Pan, X., Zhou, X., & Shi, B. (2021). Microdeformation monitoring by permanent scatterer GB-SAR interferometry based on image subset series with short temporal baselines: The Geheyan Dam case study. *Measurement*, 184, 109944. https://doi.org/10.1016/j.measurement.2021.109944

Wang, T., Perissin, D., Rocca, F., & Liao, M. S. (2011). Three Gorges Dam stability monitoring with time-series InSAR image analysis. *Science China Earth Sciences*, 54(5), 720-732. https://doi.org/10.1007/s11430-010-4101-1

Yang, S., Zhang. J., Fu, L., Chen, C., Liu, Z., & Zhang W. (2023). Landslide detection using synergistic ALOS/PALSAR-2 and Sentinel-1A data in the Qinling-Daba Mountains. *Applied Sciences,* 13(21), 12080. https://doi.org/10.3390/app132112080

Zhou, W., Li, S., Zhou, Z., & Chang, X. (2016). Remote sensing of deformation of a high concrete-faced rockfill dam using InSAR: A study of the Shuibuya dam, China. *Remote sensing*, 8(3), 255. ; https://doi.org/10.3390/rs8030255